HHS Public Access

Author manuscript

Mol Biosyst. Author manuscript; available in PMC 2015 September 18.

Published in final edited form as:

Mol Biosyst. 2015 September 15; 11(10): 2717–2726. doi:10.1039/c5mb00303b.

A Genetically Amenable Platensimycin- and Platencin-Overproducer as a Platform for Biosynthetic Explorations: a Showcase of PtmO4, a Long-Chain Acyl-CoA Dehydrogenase

Jeffrey D. Rudolf[a,†], **Liao-Bin Dong**[a,†], **Tingting Huang**[a], and **Ben Shen**[a,b,c]

[a]Department of Chemistry, The Scripps Research Institute, Jupiter, FL 33458, USA

[b]Department of Molecular Therapeutics, The Scripps Research Institute, Jupiter, FL, 33458, USA

[c]Natural Products Library Initiative, The Scripps Research Institute, Jupiter, FL, 33458, USA

Abstract

Platensimycin (PTM) and platencin (PTN) are members of a new class of promising drug leads that target bacterial and mammalian fatty acid synthases. We previously cloned and sequenced the PTM and PTN gene clusters, discovered six additional PTM-PTN dual producing strains, and demonstrated the dramatic overproduction of PTM and PTN by inactivating the pathway-specific regulators *ptmR1* or *ptnR1* in four different strains. Our ability to utilize these PTM-PTN dual overproducing strains was limited by their lack of genetic amenability. Here we report the construction of *Streptomyces platensis* SB12029, a genetically amenable, in-frame Δ*ptmR1* dual PTM-PTN overproducing strain. To highlight the potential of this strain for future PTM and PTN biosynthetic studies, we created the Δ*ptmR1* Δ*ptmO4* double mutant *S. platensis* SB12030. Fourteen PTM and PTN congeners, ten of which were new, were isolated from SB12030, shedding new insights into PTM and PTN biosynthesis. $PtmO_4$, a long-chain acyl-CoA dehydrogenase, is strongly implicated to catalyze β-oxidation of the diterpenoid intermediates in to the PTM and PTN scaffolds. SB12029 sets the stage for future biosynthetic and bioengineering studies of the PTM and PTN family of natural products.

Introduction

Platensimycin (PTM) and platencin (PTN) are members of a new class of natural product antibiotics. PTM and PTN target the bacterial fatty acid synthase (FASII). PTM selectively inhibits the chain-elongation condensing enzyme FabF/FabB and PTN dually inhibits FabF/FabB and the chain-initiation condensing enzyme FabH.[1, 2] PTM is also a potent and selective inhibitor of mammalian fatty acid synthase and has become a lead compound for the treatment of diabetes.[3] PTM and PTN are comprised of two distinct scaffolds, a highly modified diterpene-derived aliphatic cage and a 3-amino-2,4-dihydroxybenzoic acid, connected by an amide bond (Fig. 1).[4, 5] While diterpenoid natural products are common

*shenb@scripps.edu; Tel: (561) 228-2456.

†J.D.R. and L.-B.D. contributed equally.

Electronic Supplementary Information (ESI) available: Strains, plasmids, primers, design and verification of mutants, NMR data, BLAST results. See DOI: 10.1039/x0xx00000x

throughout nature, with over 60,000 representatives, diterpenoids found in bacteria are limited, and highly functionalized bacterial diterpenoids are even more rare.[6] Therefore, PTM and PTN represent an excellent opportunity to investigate diterpenoid biosynthesis and functionalization in bacteria.

We previously cloned the biosynthetic gene clusters of *ptm* and *ptn* from the PTM-PTN dual producer *Streptomyces platensis* MA7327 and the PTN producer *S. platensis* MA7339, respectively (Fig. 2).[7] Recently, we discovered six additional dual PTM-PTN producing *S. platensis* strains using a high-throughput real-time PCR method and subsequent genome sequencing of two of the six strains revealed their *ptm* gene clusters are highly conserved with that of *S. platensis* MA7327 (Fig. 2).[8] Comparison of the *ptm* and *ptn* gene clusters revealed high conservation in both sequence and organization; however, a striking difference between them was the absence of a 5.4 kb cassette containing five open reading frames (ORFs) in the PTN gene cluster.[7] The five ORFs include *ptmO3*, *ptmO4*, *ptmT3*, *ptmO5*, and *ptmR3*. These genes encode an α-ketoglutarate-dependent dioxygenase, a long-chain acyl-CoA dehydrogenase, an *ent*-kaurene synthase, a P450 monooxygenase, and a hypothetical regulatory kinase, respectively. Furthermore, introduction of this "PTM" cassette into the PTN producer *S. platensis* MA7339 conferred the ability to produce both PTM and PTN and thus revealed that the PTM cassette encodes the genes necessary for PTM production in a sole PTN producer.[7]

We sought to characterize the biosynthesis of PTM and PTN by in vivo experiments. Although gene manipulations in *S. platensis* MA7327 and MA7339 were successful, the low production of intermediates and congeners in the mutants prevented the unambiguous determination of gene function. Researchers at Merck experienced similar low titer problems. They reported the isolation of numerous PTM and PTN derivatives from the wild-type strains; however, most congeners were isolated from fermentations as large as 3400 L at titers as low as 3μg L^{-1}.[9–11] To overcome these low titers, we constructed the dual PTM-PTN overproducing strains SB12001 and SB12002[12] and the PTN overproducing strain SB12600[13] by deleting the negative transcriptional regulators *ptmR1* and *ptnR1* in *S. platensis* MA7327 and MA7339, respectively. Not only were these mutants capable of PTM and PTN production up to 100-fold greater than in the wild-type strains,[12] they also produced congeners not detectable in the wild-type strains.[13, 14] Heterologous expression of the *ptn* cluster in *Streptomyces lividans* K4-114 also produced new PTN congeners as well as PTN, albeit at titers < 5 mg L^{-1}.[15]

The dual PTM-PTN overproducing strains SB12001 and SB12002 were good candidate strains for biosynthetic investigations of both PTM and PTN as the high titers could facilitate the isolation of intermediates and congeners on a practical scale. Unfortunately, both SB12001 and SB12002 were unamenable to further genetic modifications, which led us to discover alternative PTM and PTN producers.[8] Inactivation of *ptmR1* by gene replacement in one of the six new producers, *S. platensis* CB00739, afforded SB12026, a dual PTM-PTN overproducer with titers comparable to those of SB12002 and more importantly, genetic amenability.[8, 12] This mutant circumvented the technical difficulties of the original wild-type and overproducing strains and established a system to investigate the biosynthesis of the highly functionalized bacterial diterpenoids PTM and PTN.

Here we report the construction of SB12029, an in-frame Δ*ptmR1* dual PTM-PTN overproducing strain capable of additional genetic manipulations. To highlight the potential of this strain for future PTM and PTN biosynthetic studies, we created the Δ*ptmR1* Δ*ptmO4* double mutant SB12030. Fermentation of SB12030 dramatically altered the metabolic profile and produced numerous metabolites with high titers. Fourteen PTM and PTN congeners, ten of which were new, were isolated and structurally characterized. The major congeners revealed that PtmO4 is a long-chain acyl-CoA dehydrogenase responsible for catalysing β-oxidation of the diterpenoid intermediates into the PTM and PTN scaffolds. Other isolated congeners revealed new insights into the biosynthesis of PTM and PTN. Finally, overexpression of *ptmO4* in PTN-only producing strains increased the overall production of PTN.

Results and Discussion

Construction of the genetically amenable, in-frame Δ*ptmR1* PTM-PTN overproducer SB12029 providing a powerful tool for PTM and PTN bioengineering

Although engineered dual PTM-PTN overproducing strains were available,[12] our ability to further manipulate the *ptm* genes within these overproducing strains was limited by their inability to effectively sporulate. The discovery of alternative dual PTM-PTN producing strains[8] resurrected the possibility of using an overproducing strain as a model system. As previously described,[12, 13] the pathway-specific negative transcriptional regulator *ptmR1* from *S. platensis* CB00739 was targeted for gene inactivation. To construct an in-frame and markerless Δ*ptmR1* cosmid, the apramycin cassette in pBS12034, a cosmid containing the 3'-end of the *ptm* gene cluster with a Δ*ptmR1::aac(3)IV* gene replacement,[8] was excised using FLP recombinase following reported procedures,[16, 17] resulting in pBS12037. For efficient cosmid transfer during *E. coli-Streptomyces* conjugation, the backbone of pBS12037 was retrofitted with an *aadA + oriT* cassette using λRED-mediated PCR-targeting mutagenesis,[17] affording pBS12038. pBS12038 was then introduced into *S. platensis* CB00739 by *E. coli-Streptomyces* conjugation. The recombinant strain *S. platensis* SB12029 was obtained after several rounds of selection (Fig. S1 and S2).

S. platensis SB12029 was confirmed to be a dual PTM-PTN overproducing strain by fermentation under standard conditions for PTM and PTN production (Fig. 3, panel I).[8, 12] The PTM and PTN titers were comparable with those of the aforementioned overproducing strains SB12002[12] and SB12026.[8] Importantly, SB12029 sporulated extremely well on ISP4 medium, allowing additional genetic manipulations of the *ptm* gene cluster in an overproducing background.

Inactivation of *ptmO4* within an overproducing background, yielding *S. platensis* SB12030 and dramatically altering the PTM-PTN metabolic profile

The PTM cassette contains five ORFs responsible for the divergence between PTM and PTN biosynthesis.[7] One of these ORFs, *ptmO4*, encodes a predicted long-chain acyl-CoA dehydrogenase. This was a confusing prediction as acyl-CoA dehydrogenases are the first step in the β-oxidation of fatty acids[18] and there is no apparent need for an acyl-CoA dehydrogenase in the divergence of PTM from PTN. The loss of three carbons in the

diterpenoid scaffolds of PTM and PTN (both PTM and PTN contain 17 of the original 20 diterpenoid carbons), however, resembles β-oxidation in fatty acid degradation. The idea that an acyl-CoA dehydrogenase may be necessary for both PTM and PTN biosynthesis was also confounding, as the PTN-only producer *S. platensis* MA7339 does not contain a *ptmO4* homologue within its gene cluster.[7] Furthermore, heterologous expression of the *ptn* cluster in *S. lividans* successfully produced PTN,[15] suggesting all the necessary genes for PTN production are included within the *ptn* cluster.

In an effort to reveal the biosynthetic partitioning between the PTM and PTN diterpenoid scaffolds, we targeted *ptmO4* for gene inactivation. Using λRED-mediated PCR-targeting mutagenesis,[17] we replaced the *ptmO4* gene in cosmid pBS12039 with the *aac(3)IV* + *oriT* cassette affording pBS12040, introduction of which into *S. platensis* SB12029 resulted in the Δ*ptmR1* Δ*ptmO4* double mutant SB12030 (Fig. S3 and S4). Fermentation of SB12030 in the conditions mentioned above resulted in a dramatic shift in the metabolic profile as compared to SB12029 (Fig. 3, panel II). In small-scale fermentation (50 mL), SB12030 severely decreased the production of PTM and PTN. A concomitant increase of 14 congeners not previously seen in the wild-type or PTM-PTN overproducing strains were identified by LC-MS analysis. Complementation of *ptmO4* by introduction of the integrative plasmid pBS12041, which possesses *ptmO4* under the control of the strong promoter *ErmE**, into SB12030 afforded *S. platensis* SB12031 and analysis of the fermentation extract revealed that PtmO4 restored production of PTM, albeit not to the levels seen in SB12029 (Fig. 3, panel III). The production of PTN in SB12031 was unchanged compared to SB12030, suggesting that PtmO4 may be specific for PTM biosynthesis.

Isolation and structural elucidation of PTM and PTN congeners from *S. platensis* SB12030

The dramatic metabolic shift in the overproducing Δ*ptmO4* mutant encouraged a large-scale fermentation of SB12030 to isolate the newly produced congeners. Following previously reported procedures,[8, 12, 13, 15] extraction of a 3.6 L culture with Amberlite XAD-16 resin and subsequent column chromatography resulted in the isolation of 14 compounds (Fig.1). Of these 14 compounds, ten are new and four were previously isolated from engineered PTN-producing strains (**11** and **14**) or plants (**15** and **16**). Each new compound is named "platensimycin" or "platencin" for their *ent*-kaurene (PTM) or *ent*-atiserene (PTN) scaffolds with "ML" designating that these congeners were isolated from a markerless Δ*ptmR1* overproducing mutant.

Platensimycin ML1 (**3**), isolated as a colorless oil, was a major constituent from SB12030. High-resolution ESIMS (HRESIMS) analysis yielded an $[M + H]^+$ ion at *m/z* 333.2062, consistent with a molecular formula of $C_{20}H_{29}O_4$ (calculated $[M + H]^+$ ion at *m/z* 333.2060). The ^{1}H NMR spectrum showed two olefinic protons (δ 6.39, d, J = 10.5 Hz and 5.93, d, J = 10.5 Hz), an oxymethine proton (δ 4.38, br s), and three methyl signals (δ 1.37, s;1.20, d, J =7.0 Hz; and 1.10, s) (Table S4). Analysis of the ^{13}C NMR (Table S4) and HSQC spectra of **3** confirmed the presence of 20 carbon signals attributable to an α, β-unsaturated carbonyl group (δ 203.7, 154.1, and 127.7), a carboxylic acid (δ 179.2), two oxygenated carbons (δ 87.1 and 76.9), two quaternary carbons (δ 47.3 and 46.3), three methines (δ 46.5, 45.3, and 40.2), six methylenes (δ 55.2, 43.3, 41.0, 36.8, 35.2, and 23.1),

and three methyls (δ25.1, 23.5, and 17.9). These data were very similar to the ketolidemoiety of PTM (**1**). The ^{1}H–^{1}H COSY spectrum displayed cross peaks of $H_3$18/H4/$H_2$3/$H_2$2/$H_2$1 that provide da carbon connectivity identical with the previously isolated platencins SL5 and SL6.[15] This was further confirmed by the HMBC correlations from $\underline{CH_3}$ 18 to C3, C4 and C19, as well as from $\underline{CH_3}$ 20 to C1. Detailed 2D NMR (HSQC, ^{1}H–^{1}H COSY, HMBC, ROESY) analysis indicated that the other parts of **3**, including the relative configurations, were the same as those of the ketolidemoiety of the PTM. The absolute configuration of **3**, except C4, was assigned on the basis of the biosynthetic relationship to PTM. The absolute configuration at C4 of **3** was determined by esterifying **3** with (1*R*, 2*S*)- and (1*S*, 2*R*)-2-phenyl-1-cyclohexanol to afford the corresponding esters **3a** and **3b**, respectively, and calculating the $\Delta\delta_H^{RS}$ values for the α-methyl group.[19] For the esters **3a** and **3b**, the $\Delta\delta_H^{RS}$ value for the C18 methyl was − 0.100, indicating an (*S*-) configuration at C4 (Fig. S27). Thus, the structure of **3** was fully elucidated. For consistency with PTN congeners,[15]**3** was also named (4*S*)-homoplatensic acid.

Platensimycin ML2(**4**) and ML3 (**5**) had the same molecular formula of $C_{20}H_{29}O_5$ (**4**, $[M + H]^+$ ion at *m/z* 349.2013; **5**, $[M + H]^+$ ion at *m/z* 349.2016; calculated $[M + H]^+$ ion at *m/z* 349.2010) and similar ^{1}H and ^{13}C NMR spectra (Table S4), suggesting that **4** and **5** were regioisomers. Their molecular weights were 16 Da more than **3** and likely due to one additional hydroxyl group. For **4**, the hydroxyl group was linked to C15, which caused downfield shifts of 3.3 and 4.8 ppm for the adjacent carbons C16 and C8, respectively, and was further supported by key HMBC correlations of H15 (δ3.96, s) with C7 (δ151.5), C9 (δ 47.4), C14 (δ39.3), and C17 (δ19.5). For **5**, the downfield shifts of 9.3 and 5.8 ppm appeared at C13 and C8, respectively, indicating the hydroxyl group was attached at C14. This result was confirmed by key HMBC correlations of H14 (δ4.64, s) with C7 (δ153.3), C9 (δ49.2), C12 (δ40.6) and C15 (δ49.7). The crosspeak between H13 and H14 cannot be detected in the ^{1}H–^{1}H COSY spectrum likely due to their approximate 90° dihedral angles (Fig. S28).[20] The relative configurations of the hydroxyls were elucidated by detailed analysis of the ROESY spectra. ROESY correlations of H15 with H9 (δ2.67, br s) and H14 with $\underline{CH_3}$ 20 (δ1.15, s) indicated 15*R** and 14*R** configurations for **4** and **5**, respectively. The absolute configuration of **4** and **5**, including C4, was assigned on the basis of the biosynthetic relationship to **3** and PTM.

The HRESIMS of platensimycin ML4 (**6**) showed a protonated molecular ion at *m/z* 461.2650, corresponding to the molecular formula $C_{25}H_{37}N_2O_6$ (calculated $[M + H]^+$ ion at 461.2646). Analysis of the ^{13}C NMR spectrum (Table S5) indicated the existence of a glutamine moiety (δ175.7, 175.6, 53.6, 33.2, and 29.0), which was similar to homoplatensimide A.[21] The subtraction of the signals for glutamine and comparison of the remaining signals from the ^{13}C NMR spectrum of **6** with those of **3** suggested that the tetracyclic ketolides of the two molecules were identical. An amide bond was established to connect these two moieties together as deduced by an amide proton signal (δ8.76, d, J = 7.0 Hz) in the ^{1}H NMR spectrum together with HMBC correlations from the α-$\underline{CH}$ proton of the glutamine (δ5.17, m) to the carboxyl C19 (δ177.4) from the ketolide core. Thus, **6** was established as a glutamine amide of **3**.

The HRESIMS of platensimycin ML5 (**7**) afforded an $[M + H]^+$ ion at *m/z* 420.2379 consistent with a molecular formula of $C_{23}H_{34}NO_6$(calculated $[M + H]^+$ ion at *m/z* 420.2381). According to the ^1H and ^{13}C NMR data (Table S5), **7** had the same ketolide core of **3** and **6**. Compared with **6**, the glutamine moiety of **6** was replaced with a serine moiety in **7**. The existence of serine was supported by the ^1H NMR (δ5.28, m; 4.53, dd, *J* = 11.2, 4.2; 4.40, dd, *J* = 11.2, 4.2) and ^{13}C NMR (δ174.3, 63.4, 56.5) data. HMBC correlations from the α-CH proton (δ5.28, m) of serine to the C19 carboxyl suggested an amide bond connecting the two pieces together. Thus, **7** was established as a serine amide of **3**.

Platensimycin ML6 (**8**) had a molecular formula of $C_{20}H_{29}O_5$ ($[M + H]^+$ ion at *m/z* 349.2006; calculated $[M + H]^+$ ion at *m/z* 349.2010) indicative of six degrees of unsaturation and 16 mass units higher than that of **3**. One obvious difference was found in the ^{13}C NMR spectrum of **8** compared to that of **3**. The signals for the α, β-unsaturated carbonyl group disappeared with a concurrent appearance of one keto (δ209.2) and two oxomethine (δ64.4 and 56.1) carbons, suggesting that the double bond was oxygenated to two hydroxyl groups. Considering the molecular formula, the relative high-field chemical shifts of the two oxomethines in the ^{13}C NMR, and the degrees of unsaturation, one epoxide group is present in **8**. The relative configuration of the epoxide was deduced by the ROESY correlations of H7 (δ3.29, d, *J* = 3.5 Hz) with H14b (δ1.85, dd, *J* = 11.9, 4.9 Hz) and H15b (δ1.55, d, *J* = 11.2 Hz), as well as H9 (δ2.30, br s) with H15a (δ1.87, dd, *J* = 11.2, 3.5 Hz). Detailed 2D NMR (HSQC, ^1H–^1H COSY, HMBC, ROESY) data analysis indicated that the rest of compound **8** was identical to **3**.

HRESIMS analysis of platensimycin ML7 (**9**) gave an $[M + H]^+$ion at *m/z* 335.2216 consistent with a molecular formula of $C_{20}H_{31}O_4$ (calculated for $[M + H]^+$ ion at *m/z* 335.2217), which was 2 Da larger than that of **3**. The analysis of the^1H and ^{13}C NMR spectra (Table S6) indicated that **9** was an analogue of **3**. Similar to **8**, the ^{13}CNMR signals for the α, β-unsaturated carbonyl group disappeared and were replaced by a ketogroup (δ 214.9) and two methylenes (δ36.8 and 34.0) in **9**. This was the only difference found between **9** and **3** after detailed comparison of the 2D NMR (HSQC, ^1H–^1H COSY, HMBC, ROESY) spectra.

Platensimycin ML8 (**10**) had a molecular formula of $C_{23}H_{36}NO_6$ based on HRESIMS analysis ($[M + H]^+$ ion at *m/z* 422.2541; calculated $[M + H]^+$ ion at *m/z* 422.2537). Analysis of the ^1H, ^{13}C, and 2D NMR (HSQC, ^1H–^1H COSY, HMBC, ROESY) spectra (Table S6) revealed that the ketolide core of **10** was identical to **9**. Three additional carbon (δ174.5, 63.6, 56.5) and proton (δ5.36, m; 4.58, dd, *J* = 11.2, 4.2; 4.43, dd, *J* = 11.2, 4.2) signals clearly indicated the presence of a serine moiety, as in **7**. HMBC correlations from the α-CH proton (δ5.36, m) of serine to the C19 carboxyl suggested an amide bond and connected the two moieties together. Thus, compound **10** was established as a serine amide of **9**.

Along with **3**, compound **11** was a major constituent isolated from SB12030. Its ^1H and ^{13}C NMR data was identical with that of (4*S*)-homoplatencinic acid, also called platencin SL5, a known intermediate in the heterologous biosynthesis of PTN in *S. lividans* SB12606 and SB12608.[15] Similar to **3**, the stereochemistry at C4 of platencin SL5 (**11**) is in the 4*S* configuration. We isolated three additional PTN analogues including one known and two

new compounds. The known compound, **14**, was identified as platencin A4. [13] The two new compounds, platencin ML1 and ML2(**12** and **13**) had the same molecular formula of $C_{20}H_{29}O_4$ [**12**, $[M + H]^+$ ion at *m/z* 333.2066; **13**, $[M + H]^+$ ion at *m/z* 333.2052; calculated $[M + H]^+$ ion at *m/z* 333.2060]. Their molecular weights were 16 Da more than **11** and likely due to one additional hydroxyl group. For **12**, the hydroxyl group was attached to C15, which caused downfield shifts of 5.1 and 4.4 ppm for the adjacent carbons C16 and C8,[15] respectively, and was further supported by key HMBC correlations of H15 (δ4.00, s) with C7 (δ153.6), C9 (δ38.2), C12 (δ36.6), C14 (δ20.7) and C17 (δ111.2). For **13**, the downfield shifts for C13 and C8 were 12.5 and 5.5 ppm,[15] respectively, indicating the hydroxyl group was attached at C14. This result was confirmed by the ^1H–^1H COSY cross-peaks between H14 and $H_2$13 (δ2.29, ddd, *J* = 13.3, 9.8, 3.5; 1.84, m) together with key HMBC correlations of H14 (δ4.68, ddd, *J* = 9.8, 4.4, 1.4 Hz) with C7 (δ154.6) and H12 (δ 2.41, m) and $H_2$15 (δ3.31, d, *J* = 16.8 Hz; 1.79, dd, *J* = 16.8, 1.4 Hz) with C14 (δ67.4). The relative configuration of the hydroxyls was elucidated by correlations in the ROESY spectra. ROESY correlations between H15 and H9 (δ2.08, dd, *J* = 9.8, 9.8 Hz) and between H14 and $\underline{CH_3}$ 20 (δ1.08, s) indicated 15*S** and 14*R** configurations for **12** and **13**, respectively. The absolute configuration of **12** and **13** including C4 was assigned on the basis of their biosynthetic relationships to **11** and PTN.

Compounds **3** – **16** were tested for antibacterial activity against *Streptococcus aureus* ATCC25923 and *Micrococcus luteus* ATCC9431 using a standard disk diffusion assay. Consistent with the requirement of the 3-amino-2,4-dihydroxybenzoic acid moiety for activity,[22] none of the isolated PTM or PTN congeners showed antibacterial activity.

ptmO4, encoding a long-chain acyl-CoA dehydrogenase, catalysing β-oxidation of the diterpenoid intermediates into the PTM and PTN scaffolds

Each of the isolated compounds had all 20 of its diterpenoid carbons, indicating that *ptmO4* acts before the presumptive thiolytic loss of a propyl moiety in PTM and PTN biosynthesis. Interestingly, all but two (**15** and **16**) of the isolated congeners have open A rings with single bonds connecting C3 and C4 (Fig. 1). This strongly implies that PtmO4, a putative long-chain acyl-CoA dehydrogenase, is responsible for the formation of the double bond between C3 and C4. The formation of this double bond in PTM and PTN biosynthesis is analogous to the first step in the β-oxidation cycle in fatty acid degradation.[18] The CoA derivatives of the two major compounds isolated, **3** and **11**, are predicted to be the substrates for the PtmO4 dehydrogenation reaction due to their high accumulation. All of the other congeners (**4** – **10, 12 – 14**) with open A rings are presumably shunt metabolites from the accumulated **3** or **11** that have been aminoacylated by amino acids present during fermentation or oxidized by adventitious enzymes such as P450s (Figs. 1 and 4).

Overexpression of *ptmO4* in PTN-only producing strains improving the production of PTN

With new evidence supporting PtmO4 as one enzyme that processes both scaffolds of PTM and PTN, we were intrigued how PTN is processed in the absence of a *ptmO4* homologue. The PTN-only producer *S. platensis* MA7339 and the heterologous PTN-production strains *S. lividans* SB12606 and SB12608 do not contain the PTM cassette, and therefore lack *ptmO4*.[7, 15] In large-scale fermentation of SB12030, the overproducing Δ*ptmO4* mutant,

small amounts of PTM and PTN (<1 mg L^{-1}) were isolated. In comparison, the Δ*ptmR1* dual PTM-PTN overproducing strain SB12029 produces >300 and 150 mg L^{-1}, respectively. Given the high concentrations of **3** and **11** during fermentation and that long-chain acyl-CoA dehydrogenases are involved in primary metabolism, it is conceivable that a *ptmO4* homologue outside the gene cluster is responsible for the limited processing of the PTM and PTN scaffolds in the Δ*ptmO4* mutant. In fact, a BLAST[23] search of *ptmO4* against the genome of *S. platensis* CB00739[8] revealed 16 homologues with >90% coverage of varying homology (28 – 53% identity, 42–69% similarity, Table S9). A similar mechanism occurring in the PTN-only producing strains MA7339, SB12606, and SB12608 is also possible.

PTN is commonly produced at a much lower titer than PTM in dual PTM-PTN producers and overproducers[8, 12] and the PTN overproducing strain SB12600[13] produces ca. 10-fold less PTN than in the dual PTM-PTN overproducing strains.[8] In *S. lividans* SB12606 and SB12608, **11**, was produced ca. 7-fold more than PTN.[15] Although these facts are circumstantial, and four other genes from the PTM cassette are also missing in these strains, we sought to determine whether the lack of *ptmO4* in these strains prevents complete processing of the diterpenoid intermediate into the PTN scaffold.

The replicative plasmid, pBS12042, overexpressing *ptmO4*, was introduced into *S. lividans* SB12606 and SB12608 to afford *S. lividans* SB12614 and SB12615, respectively, by *E. coli-Streptomyces* conjugal transfer. Fermentation of these PTN-only producing strains containing *ptmO4* under the control of the strong promoter *ErmE** resulted in a modest improvement of PTN production and concomitant decrease in **11**, the implicated substrate of PtmO4 (Fig. 3, panels IV and V). The appearance of a hydroxylated analogue of PTN was also evident in *S. lividans* SB12614 and SB12615, suggesting an excess of PTN available for adventitious hydroxylation. It is evident that PtmO4 contributes to both PTM and PTN production. The lack of a *ptmO4* homologue within the *ptn* gene cluster suggests that sole PTN producers are dependent on substrate flexible acyl-CoA dehydrogenases elsewhere in the genome for complete biosynthesis of PTN.

Isolated congeners revealing new insights into PTM and PTN biosynthesis

We initially proposed a unified pathway for PTM and PTN biosynthesis.[7] This pathway proposed (i) *ent*-copalyl diphosphate (*ent*-CPP) is the final common intermediate in PTM and PTN biosynthesis, (ii) dedicated diterpene synthases, *ent*-kaurene synthase (PtmT3) and *ent*-atiserene synthase (PtmT1), control the divergence between PTM and PTN, respectively, (iii) a select group of enzymes specific to PTM and presumably in the PTM cassette form the characteristic ether linkage of PTM, (iv) a group of enzymes to oxidatively tailor the scaffolds of both PTM and PTN to form platensicyl- or platencinyl-CoA, and (v) an amide coupling reaction with 3-amino-2,4-dihydroxybenzoic acid to complete the biosynthesis of both PTM and PTN. Heterologous expression of PTN and its congeners within *S. lividans* revealed (i) oxidation at C19, and possibly CoA activation, precedes ring cleavage, (ii) hydroxylation at C7 sets up enone formation, and (iii) a possible retro-aldol cleavage of the A ring may result in uncontrolled stereospecificity at C4.[15] The isolation of PTM and PTN congeners from *S. platensis* SB12030 supports a unified pathway for PTM and PTN

biosynthesis and further reveals biosynthetic steps and timing of PTM and PTN biosynthesis.

As discussed earlier, **3** and **11** are strongly implicated as substrates for PtmO4. PtmO4 is proposed to catalyze β-oxidation of the diterpenoid intermediates, resulting in thiolysis of three carbons, for both PTM and PTN scaffolds (Fig. 4). The consistent stereochemistry at C4 of **3** and **11**, along with all the other open A ring congeners (**4 – 10, 12 – 14**), are consistent with our unified pathway hypothesis where one set of genes – *ptm* and *ptn* – encode enzymes that process both scaffolds of PTM and PTN. The proposed retro-aldol cleavage of the C4/C5 bond to open the A ring results in a stereospecific formation of (*S*)-C4.

As seen in PTN biosynthesis in *S. lividans*,[15] oxidation at C19 also occurs early in PTM biosynthesis. Isolation of **15** and **16** suggests that C19 oxidation precedes ether ring formation. The early steps in PTM biosynthesis therefore resemble gibberellin biosynthesis in plants, fungi, and plant growth promoting bacteria.[24, 25] Comparisons between the C19 oxidations in PTM and PTN biosynthesis and gibberellin biosynthesis indeed reveal both similarities and differences. Thus, in gibberellin biosynthesis, *ent*-CPP is cyclized to *ent*-kaurene, which undergoes sequential oxidations at C19 and C7 to form (7*S*)-*ent*-kaur-16-en-7-ol-19-oic acid.[24] In PTM biosynthesis *ent*-CPP is proposed to be cyclized into (16*R*)-*ent*-kauran-16-ol, C19 oxidation of which then occurs before ether ring formation. Since C11 and C16 in the ether linkage of PTM are both *S* configurations,[4] isolation of **15** and **16** from SB12030 suggests that the 11*S*, 16*S*-ether ring is formed from a (16*R*)-hydroxyl precursor. It is conceivable that hydroxylation at C11 results in an 11*S*, 16*R*-diol intermediate, which then can undergo ether formation to afford **16**. A similar transformation was seen in the fungus *Gibberella fujikuroi*, albeit in the absence of C19 oxidation.[26] The P450 monooxygenase and α-ketoglutarate-dependent dioxygenase found within the PTM cassette, PtmO5 and PtmO3, respectively, are likely candidates given this transformation occurs only in PTM.

We previously isolated PTN SL4, an *ent*-atiseren-19-oic acid derivative with a hydroxyl at C7, suggesting a hydroxylation and dehydration sequence to account for formation of theenone moiety of PTN.[15] Following the unified biosynthetic pathway, a similar hydroxylation at C7 of **16** could be proposed for PTM; however, the isolation of **9** and **10** may suggest that C7 hydroxylation occurs after retro-aldol ring cleavage. On the other hand, isolation of **8** could be attributed to adventitious oxidation of **3** accumulated in SB12030.

In sum, based on congeners isolated in this study, as well as previous studies, we now propose that *ent*-CPP is first cyclised to (16*R*)-*ent*-kauran-16-ol, which is then oxidized to (16*R*)-*ent*-kauran-16-ol-19-oic acid via **15**, directly followed by ether ring formation to **16**. Subsequent hydroxylation at C7, retro-aldol ring cleavage at C4 and C5, and dehydration at C6 and C7 afford the diterpenoid intermediate **3**. PtmO4 next catalyzes β-oxidation of **3**, most likely in its CoA form, to yield the corresponding α,β-unsaturated product, the intermediacy of which is supported by the isolation of homoplatensimide A.[21] Subsequent processing of the α,β-unsaturated sidechain by hydration, oxidation, and thiolytic loss of a

propyl moiety afford splatensicyl-CoA, which is finally coupled with 3-amino-2,4,-dihydroxybenzoic acid to yield PTM (Fig. 4).

Conclusions

PTM and PTN hold a treasure-trove of undiscovered biosynthetic information due to their highly functionalized nature and the rarity of diterpenoid natural products currently known in bacteria. PTM and PTN have both similarities and differences to diterpenoid biosynthesis in plants and fungi. Similarities with diterpenoid biosynthesis in plants and fungi present an opportunity to address unanswered questions in more feasible bacteria model systems while differences allow the discovery of novel biochemistries and enzymes. The construction of genetically amenable and dual PTM-PTN overproducing strains provides a platform to explore PTM and PTN biosynthesis. The construction of this system not only facilitates genetic manipulation and the isolation of congeners as shown in this study, it sets the stage for the continued bioengineering of the *ptm* cluster, substrate generation for in vitro applications including enzymology and structural biology, and combinatorial chemistry for natural product structural diversity featuring the PTM and PTN scaffolds.

Experimental

General experimental procedures

All ^{1}H, ^{13}C, and 2D NMR (HSQC, ^{1}H–^{1}H COSY, HMBC, ROESY) spectra were collected with a Bruker Avance III Ultrashield 700 at 700 MHz for ^{1}H and 175 MHz for ^{13}C nuclei. MPLC separation was performed using a Biotage Isolera One using a Biotage SNAP Cartridge HP-Sil column (60 g). Preparative HPLC was carried out on an Agilent 1260 Infinity LC equipped with an Agilent Eclipse XDB-C18 column (250 mm × 21.2 mm, 7 μm). LC-MS was conducted using an Agilent 1260 Infinity LC coupled to a 6230 TOF (HRESI) equipped with an Agilent Poroshell 120 EC-C18 column (50 mm × 4.6 mm, 2.7 μm). Optical rotations were measured using an AUTOPOL IV automatic polarimeter (Rudolph Research Analytical). UV spectra were obtained with a NanoDrop 2000C spectrophotometer (Thermo Scientific).

Bacterial strains, plasmids, biochemicals, and culture conditions

Strains, plasmids, and polymerase chain reaction (PCR) primers used in this study are summarized in Tables S1-S3, respectively. *E. coli* DH5α was used for general subcloning and plasmid or cosmid preparation.[27] PCR primers were synthesized by Sigma-Aldrich. All restriction endonucleases, Q5 high-fidelity DNA polymerase, and T4 DNA ligase were purchased from NEB and the reactions were performed according to the manufacturer's procedures. Commercial kits (Omega Bio-Tek) were used for gel extraction and plasmid preparation. DNA sequencing was performed by Eton Bioscience. The REDIRECT Technology kit for λRED-mediated PCR-targeting mutagenesis was provided by the John Innes Center (Norwich, UK).[17] *E. coli* ET12567/pUZ8002[28] was used as the *E. coli* host for intergeneric conjugation. pJTU2170 and pUWL201PWT were used as the shuttle vectors for gene complementations. pUWL201PWT is a derivative of pUWL201PW[29] containing an *oriT* sequence that was cloned into its *Pst* I site. *S. platensis* CB00739 and pBS12034,[8] and

S. lividans SB12606 and SB12608[15] were reported previously. Other common biochemicals and media components were purchased from standard commercial sources and used directly.

E. coli strains containing plasmids or cosmids were grown in lysogeny broth (LB) with appropriate antibiotic selection.[27] *Streptomyces* strains were cultured in liquid tryptic soy broth (TSB) or solid ISP4 medium with appropriate antibiotic selection.[30] *E. coli-Streptomyces* conjugations were performed on solid ISP4 freshly supplemented with 10 mM $MgCl_2$. Fermentation of *S. platensis* recombinant strains followed previously reported protocols.[7, 8, 12] Briefly, *Streptomyces* spp. spores were inoculated into seed medium and incubated at 28 °C and 250 rpm for 2 d. PTM fermentation medium was inoculated with 4% (v/v) seed culture and 3% (w/v) Amberlite XAD-16 resin (Sigma-Aldrich) and cultured at 28 °C and 250 rpm for 7 d.

Construction of the *S. platensis* PTM-PTN overproducing recombinant strain SB12029

To construct an in-frame Δ*ptmR1* cosmid, pBS12034,[8] a cosmid containing the 3'-end of the *ptm* gene cluster with a Δ*ptmR1::aac(3)IV* gene replacement, was subjected to FLP-mediated cassette excision by its introduction into *E. coli* DH5α/BT340.[16] Following reported procedures,[17] overnight incubation at 42 °C resulted in loss of the *aac(3)IV* cassette and generation of an 81 bp scar, affording pBS12037. The Supercos 1 backbone of pBS12037 was then modified to include an *oriT* sequence for integration into *Streptomyces*. A 511 bp noncoding region of the backbone of pBS12037 was replaced with the *aadA-oriT* cassette from pIJ778 using λRED-mediated PCR-targeting mutagenesis in *E. coli* BW25113/pIJ790 (Table S3).[17] The genotype of the resultant cosmid, pBS12038, was confirmed by PCR analysis using primers oriT_ID_F and oriT_ID_R and restriction enzyme digestion. pBS12038 was transformed into the nonmethylating *E. coli* ET12567/pUZ8002[28] and introduced into *S. platensis* CB00739[8] by intergeneric conjugation, as previously described.[17] Single crossovers of Δ*ptmR1* were selected for by kanamycin resistance on ISP4 medium. After several rounds of passaging the single-crossover exconjugants in liquid TSB and solid ISP4 media, double-crossover mutants, which were kanamycin sensitive, were obtained. The in-frame and markerless Δ*ptmR1* mutant, *S. platensis* SB12029, was confirmed by PCR analysis using primers 739R1ID_F and 739R1ID_R (Fig. S1) and Southern analysis (Fig. S2).

Inactivation and complementation of *ptmO4* (long-chain acyl-CoA dehydrogenase)

Gene replacement of *ptmO4* was performed in *E. coli* BW25113/pIJ790 carrying pBS12039, a cosmid containing a partial *ptm* gene cluster but not *ptmR1*, by λRED-mediated PCR-targeting as described above (Table S3). The *ptmO4* gene was replaced with the *aac(3)IV* + *oriT* cassette from pIJ773[17] resulting in pBS12040. pBS12040 was introduced into *S. platensis* SB12029 by *E. coli-Streptomyces* conjugation as described above. Double-crossover mutants were selected for by apramycin resistance and kanamycin sensitivity. The *ptmO4* mutation in *S. platensis* SB12030 was confirmed by PCR analysis using primers 739O4ID_F and 739O4ID_R (Fig. S3) and Southern analysis (Fig. S4).

The *ptmO4* gene from *S. platensis* CB00739 was amplified by PCR using Q5 high-fidelity DNA polymerase and cloned into the *Nde*I and *Xba*I sites of the pJTU2170 *E. coli-*

Streptomyces expression shuttle vector[31] behind the *ErmE** strong promoter. For complementation of *ptmO4* into the heterologous PTN producers, the *ptmO4* gene was cloned into the *Nde*I and *Bam*HI sites of the pUWL201PWT *E. coli-Streptomyces* expression shuttle vector[29] behind the *ErmE** strong promoter. The complementation plasmids, pBS12041 and pBS12042, were introduced into *S. platensis* SB12030, and *S. lividans* SB12606 and SB12608,[15] to afford SB12031, SB12614, and SB12615, respectively, using the procedures described above. Strains containing the pBS12041 or pBS12042 complementation vectors were selected for using kanamycin or thiostrepton resistance, respectively.

Extraction and isolation

Extraction of resin from small-scale fermentations followed previously reported protocols.[8, 12] After fermentation of the recombinant *Streptomyces* strains, the resin was harvested by centrifugation, washed three times with H_2O, and extracted three times with methanol. Methanol was removed by rotary evaporation and the resulting oil was resuspended in methanol prior to analysis. Liquid chromatography for LC-MS analysis was performed using an 18 min solvent gradient (0.4 mL min^{-1}) from 5% – 100% CH_3CN containing 0.1% formic acid in H_2O containing 0.1% formic acid.

For large-scale fermentation (3.6 L) of SB12030, nine 2.0-L baffled flasks containing 400 mL medium containing 4% (v/v) seed culture were prepared. Following the 7-day fermentation, there sin was separated from broth and cells by centrifugation. After drying for 24 h, the resin was extracted three times with ca. 500 mL of methanol. The methanol was removed under reduced pressure and the crude extract (4.8 g) was adsorbed to C18 reverse phase resin (Biotage) and fractionated by MPLC eluting with a gradient of CH_3OH−H_2O (30:70, 60:40, 80:20, and 100:0) to give four fractions (Fr01–Fr04). Since the major constituents of Fr04 were fatty acids, no further purification of Fr04 was carried out. Compound **11** (220 mg) was the major constituent of Fr03, which was easily purified by silicagel column chromatography using an isocratic elution system of CH_2Cl_2−CH_3OH (90:10). The remaining residue of Fr03 was combined and purified by preparative reversed-phase HPL Cusing a 30 min solvent gradient elution from 30% to 100% CH_3CN in H_2O containing 0.1% formic acid to obtain **15** (5.6 mg) and **16** (20 mg). Fraction Fr02 was chromatographed on a Sephadex LH-20 column using pure methanol as the mobile phase to generate three subfractions (Fr0201–Fr0203). Subfraction Fr0202 was further chromatographed on preparative reversed-phase HPLC using a gradient elution system of 30% to 100% CH_3CN in H_2O containing 0.1% formic acid and using LC-MS to track the compounds with no UV absorption to afford a pure natural product (**3**, 300 mg) and four other subfractions (Fr020201–Fr020204). Compound **13** (2.6 mg) was isolated from Fr020201 using preparative reversed-phase HPLC with a gradient elution of 30% to 100% methanol. Subfractions Fr020202–Fr020204 were each run on a preparative reversed-phase HPLC using a gradient solvent system of 30% to 60% CH_3CN in 0.1% H_2O containing formic acid to obtain **12** (8.6 mg), **9** (10.1 mg), and **8** (1.9 mg), respectively. Subfraction Fr0203 was chromatographed on a preparative reversed-phase HPLC using the conditions for Fr020202–Fr020204 to furnish **14** (20.5 mg). Fraction Fr01 was fractionated by a preparative reversed-phase HPLC using an elution system of 10% to 50%CH_3CN in H_2O

containing 0.1% formic acid to provide the subfractions Fr0101–Fr0103. Subfraction F0102 was further chromatographed over a preparative reversed-phase HPLC column using an isocratic elution of 24% CH_3CN in H_2O containing 0.1% formic acid to give **5** (36.8 mg). The identical solvent system was used for preparative reversed-phase HPLC of the subfraction Fr0103 to yield **4** (3.8 mg), **6** (10.0 mg), **7** (46.3 mg), and **10** (7.2 mg).

Platensimycin ML1 (3)—Colorless oil; $[\alpha]_D^{26} -33.7$ (c 5.64, CH_3OH); UV (DMSO) λ_{max} (log ε) 252 (2.73) nm; ^1H and ^{13}C NMR data, see Table S4; HRESIMS affording the $[M + H]^+$ ion at *m/z* 333.2062 (calculated $[M + H]^+$ ion for $C_{20}H_{29}O_4$ at *m/z* 333.2060).

Platensimycin ML2 (4)—Colorless oil; $[\alpha]_D^{26} +19.2$ (c 0.38, CH_3OH); UV (DMSO) λ_{max} (log ε) 250 (2.62) nm; ^1H and ^{13}C NMR data, see Table S4; HRESIMS affording the $[M + H]^+$ ion at *m/z* 349.2013 (calculated $[M + H]^+$ ion for $C_{20}H_{29}O_5$ at *m/z* 349.2010).

Platensimycin ML3 (5)—Colorless oil; $[\alpha]_D^{26} 109.7$ (c 0.74, CH_3OH); UV (DMSO) λ_{max} (log ε) 251 (2.74) nm; ^1H and ^{13}C NMR data, see Table S4; HRESIMS affording the $[M + H]^+$ ion at *m/z* 349.2016 (calculated $[M + H]^+$ ion for $C_{20}H_{29}O_5$ at *m/z* 349.2010).

Platensimycin ML4 (6)—Colorless oil; $[\alpha]_D^{26} -23.6$ (c 0.50, CH_3OH); UV (DMSO) λ_{max} (log ε) 251 (2.64) nm; ^1H and ^{13}C NMR data, see Table S5; HRESIMS affording the $[M + H]^+$ ion at *m/z* 461.2650 (calculated $[M + H]^+$ ion for $C_{25}H_{37}N_2O_6$ at *m/z* 461.2646).

Platensimycin ML5 (7)—Colorless oil; $[\alpha]_D^{26} -24.3$ (c 0.92, CH_3OH); UV (DMSO) λ_{max} (log ε) 252 (2.65) nm; ^1H and ^{13}C NMR data, see Table S5; HRESIMS affording the $[M + H]^+$ ion at *m/z* 420.2379 (calculated $[M + H]^+$ ion for $C_{23}H_{34}NO_6$ at *m/z* 420.2381).

Platensimycin ML6 (8)—Colorless oil; $[\alpha]_D^{26} -31.6$ (c 0.19, CH_3OH); ^1H and ^{13}C NMR data, see Table S5; HRESIMS affording the $[M + H]^+$ ion at *m/z* 349.2006 (calculated $[M + H]^+$ ion for $C_{20}H_{29}O_5$ at *m/z* 349.2010).

Platensimycin ML7 (9)—Colorless oil; $[\alpha]_D^{26} -27.1$ (c 0.51, CH_3OH); ^1H and ^{13}C NMR data, see Table S6; HRESIMS affording the $[M + H]^+$ ion at *m/z* 335.2216 (calculated $[M + H]^+$ ion for $C_{20}H_{31}O_4$ at *m/z* 335.2217).

Platensimycin ML8 (10)—Colorless oil; $[\alpha]_D^{26} -13.3$ (c 0.36, $MeCH_3OHOH$); ^1H and ^{13}C NMR data, see Table S6; HRESIMS affording the $[M + H]^+$ ion at *m/z* 422.2541 (calculated $[M + H]^+$ ion for $C_{23}H_{36}NO_6$ at *m/z* 422.2537).

(4*S*)-Homoplatencinic acid (11)—The NMR data matched the literature.[15]

Platencin ML1 (12)—Colorless oil; $[\alpha]_D^{26} -15.1$ (c 0.43, CH_3OH); UV (DMSO) λ_{max} (log ε) 252 (2.52) nm; ^1H and ^{13}C NMR data, see Table S7; HRESIMS affording the $[M + H]^+$ ion at *m/z* 333.2066 (calculated $[M + H]^+$ ion for $C_{20}H_{29}O_4$ at *m/z* 333.2060).

Platencin ML2 (13)—Colorless oil; $[\alpha]_D^{26} - 80.8$ (c 0.26, CH_3OH); UV (DMSO) λ_{max} (log ε) 252 (2.59) nm; ^1H and ^{13}C NMR data, see Table S7; HRESIMS affording the $[M + H]^+$ ion at *m/z* 333.2052 (calculated $[M + H]^+$ ion for $C_{20}H_{29}O_4$ at *m/z* 333.2060).

Platencin A4 (14)—The NMR data matched the literature.[13]

(16*R*)-*ent*-kauran-16,19-diol (15)—The NMR data matched the literature.[32]

(11*S*,16*S*)-*ent*-kauran-11,16-epoxy-19-oic acid (16)—The NMR data matched the literature.[33]

Antibacterial assay

The antibacterial activities of compounds **3** – **16** were tested against *Streptococcus aureus* ATCC25923 and *Micrococcus luteus* ATCC9431 using a standard disk diffusion assay. Quantities of compounds **3 – 16** (20μg) in DMSO were applied to 7 mm paper disks (Whatman) and dried. PTM (**1**) and PTN (**2**) (5μg) in DMSO were used as positive controls. The disks were placed onto solid LB agar plates applied with dense bacterial liquid cultures (ca. 18 h). The plates were incubated overnight at 37 °C and zones of inhibition, if any, were subsequently observed.

Supplementary Material

Refer to Web version on PubMed Central for supplementary material.

Acknowledgements

We thank the John Innes Center, Norwich, UK, for providing the REDIRECT Technology kit. This work is supported in part by the Natural Products Library Initiative at TSRI and NIH Grant AI079070.

Notes and references

1. Wang J, Soisson SM, Young K, Shoop W, Kodali S, Galgoci A, Painter R, Parthasarathy G, Tang YS, Cummings R, Ha S, Dorso K, Motyl M, Jayasuriya H, Ondeyka J, Herath K, Zhang C, Hernandez L, Allocco J, Basilio A, Tormo JR, Genilloud O, Vicente F, Pelaez F, Colwell L, Lee SH, Michael B, Felcetto T, Gill C, Silver LL, Hermes JD, Bartizal K, Barrett J, Schmatz D, Becker JW, Cully D, Singh SB. Nature. 2006; 441:358–361. [PubMed: 16710421]
2. Wang J, Kodali S, Lee SH, Galgoci A, Painter R, Dorso K, Racine F, Motyl M, Hernandez L, Tinney E, Colletti SL, Herath K, Cummings R, Salazar O, Gonzalez I, Basilio A, Vicente F, Genilloud O, Pelaez F, Jayasuriya H, Young K, Cully DF, Singh SB. Proc. Natl. Acad. Sci. USA. 2007; 104:7612–7616. [PubMed: 17456595]
3. Wu M, Singh SB, Wang J, Chung CC, Salituro G, Karanam BV, Lee SH, Powles M, Ellsworth KP, Lassman ME, Miller C, Myers RW, Tota MR, Zhang BB, Li C. Proc. Natl. Acad. Sci. USA. 2011; 108:5378–5383. [PubMed: 21389266]
4. Singh SB, Jayasuriya H, Ondeyka JG, Herath KB, Zhang C, Zink DL, Tsou NN, Ball RG, Basilio A, Genilloud O, Diez MT, Vicente F, Pelaez F, Young K, Wang J. J. Am. Chem. Soc. 2006; 128:11916–11920. [PubMed: 16953632]
5. Jayasuriya H, Herath KB, Zhang C, Zink DL, Basilio A, Genilloud O, Diez MT, Vicente F, Gonzalez I, Salazar O, Pelaez F, Cummings R, Ha S, Wang J, Singh SB. Angew. Chem., Int. Ed. 2007; 46:4684–4688.

6. Smanski MJ, Peterson RM, Huang S-X, Shen B. Curr. Opin. Chem. Biol. 2012; 16:132–141. [PubMed: 22445175]
7. Smanski MJ, Yu Z, Casper J, Lin S, Peterson RM, Chen Y, Wendt-Pienkowski E, Rajski SR, Shen B. Proc. Natl. Acad. Sci. USA. 2011; 108:13498–13503. [PubMed: 21825154]
8. Hindra, Huang T, Yang D, Rudolf JD, Xie P, Xie G, Teng Q, Lohman JR, Zhu X, Huang Y, Zhao L-X, Jiang Y, Duan Y, Shen B. J. Nat. Prod. 2014; 77:2296–2303. [PubMed: 25238028]
9. Zhang C, Ondeyka J, Dietrich L, Gailliot FP, Hesse M, Lester M, Dorso K, Motyl M, Ha SN, Wang J, Singh SB. Bioorg. Med. Chem. 2010; 18:2602–2610. [PubMed: 20299229]
10. Zhang C, Ondeyka J, Guan Z, Dietrich L, Burgess B, Wang J, Singh SB. J. Antibiot. 2009; 62:699–702. [PubMed: 19911028]
11. Singh SB, Ondeyka JG, Herath KB, Zhang C, Jayasuriya H, Zink DL, Parthasarathy G, Becker JW, Wang J, Soisson SM. Bioorg. Med. Chem. Lett. 2009; 19:4756–4759. [PubMed: 19581087]
12. Smanski MJ, Peterson RM, Rajski SR, Shen B. Antimicrob. Agents Chemother. 2009; 53:1299–1304. [PubMed: 19164156]
13. Yu Z, Smanski MJ, Peterson RM, Marchillo K, Andes D, Rajski SR, Shen B. Org. Lett. 2010; 12:1744–1747. [PubMed: 20232845]
14. Yu Z, Rateb ME, Smanski MJ, Peterson RM, Shen B. J. Antibiot. 2013; 66:291–294. [PubMed: 23361357]
15. Smanski MJ, Casper J, Peterson RM, Yu Z, Rajski SR, Shen B. J. Nat. Prod. 2012; 75:2158–2167. [PubMed: 23157615]
16. Cherepanov PP, Wackernagel W. Gene. 1995; 158:9–14. [PubMed: 7789817]
17. Gust B, Challis GL, Fowler K, Kieser T, Chater KF. Proc. Natl. Acad. Sci. USA. 2003; 100:1541–1546. [PubMed: 12563033]
18. Kunau W-H, Dommes V, Schulz H. Prog. Lipid Res. 1995; 34:267–342. [PubMed: 8685242]
19. Ferreiro MJ, Latypov SK, Quinoa E, Riguera R. J. Org. Chem. 2000; 65:2658–2666. [PubMed: 10808438]
20. Dong L-B, Yang J, He J, Luo H-R, Wu X-D, Deng X, Peng L-Y, Cheng X, Zhao Q-S. Chem. Comm. 2012; 48:9038–9040. [PubMed: 22854533]
21. Jayasuriya H, Herath KB, Ondeyka JG, Zink DL, Burgess B, Wang J, Singh SB. Tet. Lett. 2008; 49:3648–3651.
22. Nicolaou KC, Stepan AF, Lister T, Li A, Montero A, Tria GS, Turner CI, Tang Y, Wang J, Denton RM, Edmonds DJ. J. Am. Chem. Soc. 2008; 130:13110–13119. [PubMed: 18771264]
23. Altschul SF, Gish W, Miller W, Myers EW, Lipman DJ. J. Mol. Biol. 1990; 215:403–410. [PubMed: 2231712]
24. Boemke C, Tudzynski B. Phytochemistry. 2009; 70:1876–1893. [PubMed: 19560174]
25. Bottini R, Cassan F, Piccoli P. Appl. Microbiol. Biotechnol. 2004; 65:497–503. [PubMed: 15378292]
26. Fraga BM, Gonzalez P, Guillermo R, Hernandez MG. Nat. Prod. Lett. 1996; 8:257–262.
27. Sambrook, J.; Russel, D. Molecular cloning: A Laboratory Manual. 3rd Ed. Cold Spring Harbor, NY: Cold Spring Harbor Laboratory Press; 2001.
28. MacNeil DJ, Gewain KM, Ruby CL, Dezeny G, Gibbons PH, MacNeil T. Gene. 1992; 111:61–68. [PubMed: 1547955]
29. Doumith M, Weingarten P, Wehmeier UF, Salah-Bey K, Benhamou B, Capdevila C, Michel JM, Piepersberg W, Raynal MC. Mol. Gen. Genetics. 2000; 264:477–485.
30. Kieser, T.; Bibb, MJ.; Buttner, MJ.; Chater, KF.; Hopwood, DA. Practical Streptomyces Genetics. Norwich, UK: The John Innes Foundation; 2000.
31. Chen W, Dai D, Wang C, Huang T, Zhai L, Deng Z. Microb. Cell Factories. 2013; 12:121.
32. Satake T, Murakami T, Saiki Y, Chen CM. Chem. Pharma. Bull. 1983; 31:3865–3871.
33. Murakami T, Iida H, Tanaka N, Saiki Y, Chen C-M, Iitaka Y. Chem. Pharm. Bull. 1981; 29:657–662.

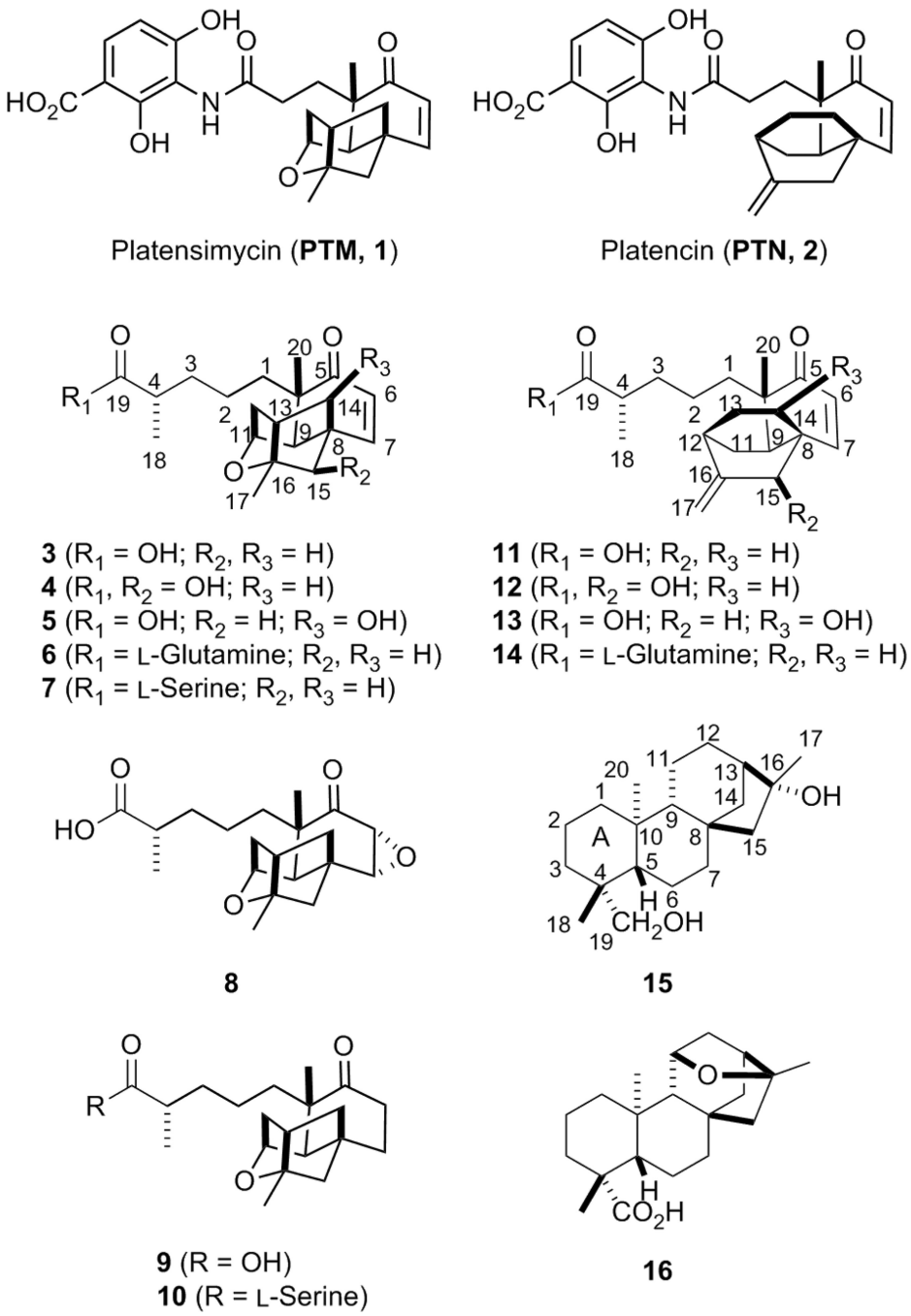

Fig. 1.

Structures of PTM (**1**), PTN (**2**), new (**3 – 10, 12, 13**), and known congeners (**11, 14 – 16**) isolated from the recombinant strain *S. platensis* SB12030. The major constituents of SB12030 were **3** and **11**.

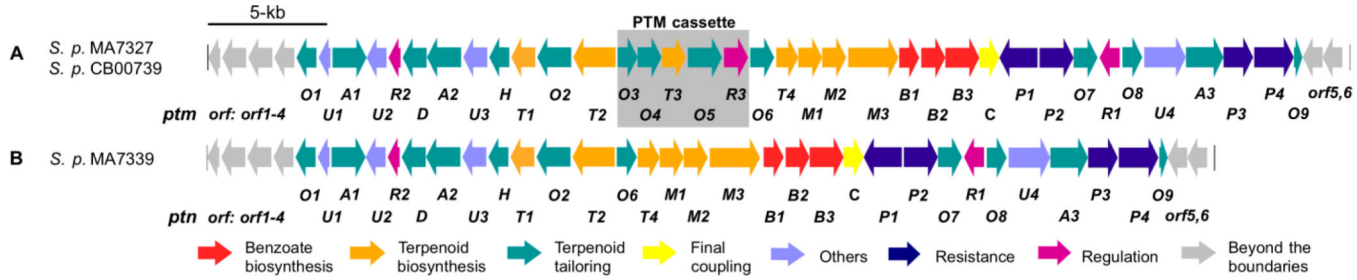

Fig. 2.

The *ptm* and *ptn* biosynthetic gene clusters. (A) Genetic organization of the *ptm* gene clusters from *S. platensis* MA7327 and CB00739 and (B) the *ptn* gene cluster from *S. platensis* MA7339. The PTM cassette, which contains five ORFs including *ptmO4*, is present in the *ptm* cluster yet absent in the *ptn* cluster.

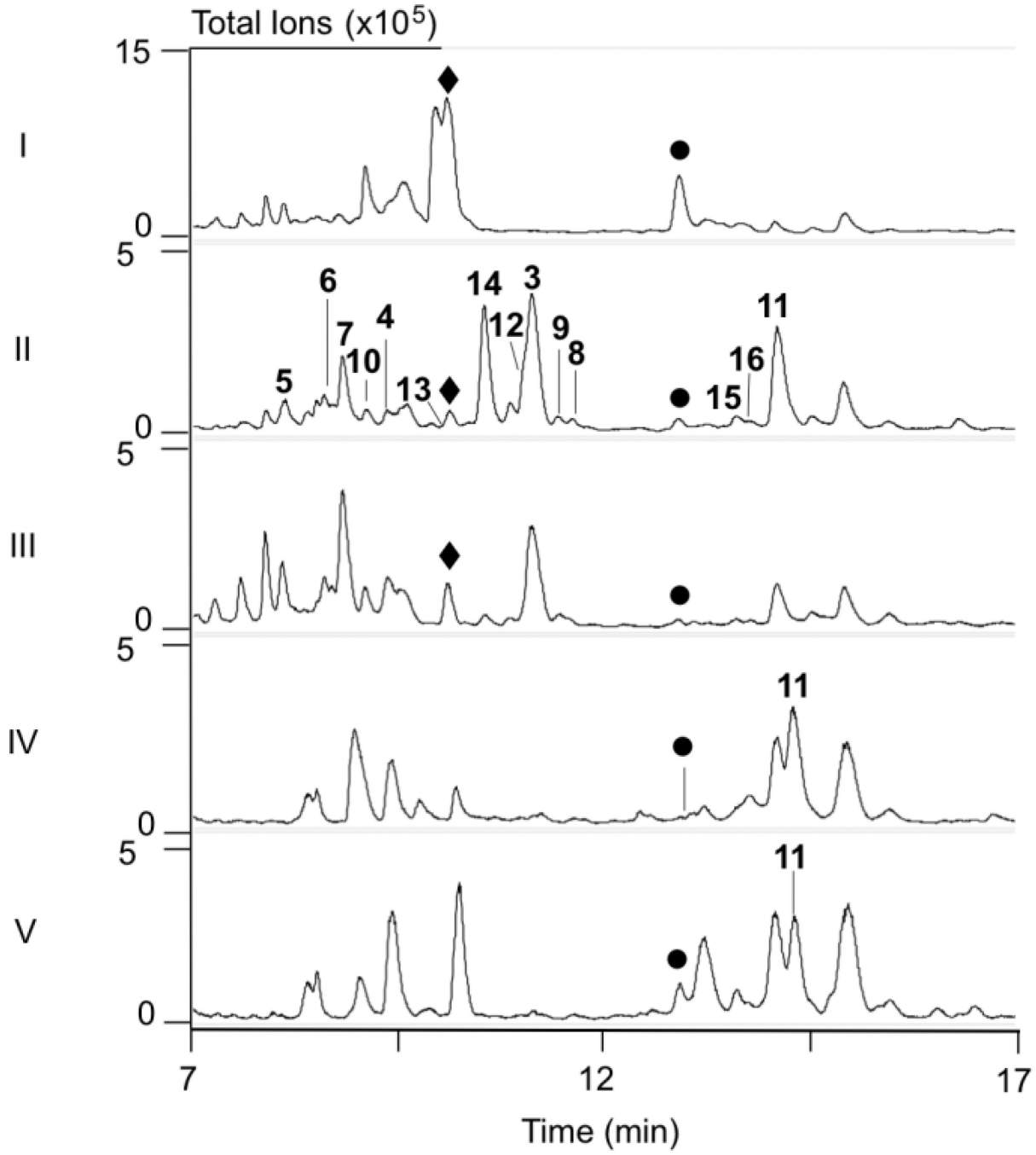

Fig. 3.

LC-MS analysis of *S. platensis* and *S. lividans* recombinant strains. Crude extracts of each strain were analyzed using total ion chromatograms (TICs). (I) SB12029 (CB00739 Δ*ptmR1*); (II) SB12030 (SB12029 Δ*ptmO4*); (III) SB12031 (SB12030 + *ptmO4*); (IV) SB12606 or SB12608(*S. lividans* + *ptn* cluster Δ*ptnR1*); (V) SB12614 or SB12615 (SB12606 or SB12608 + *ptmO4*). (♦) PTM; (●) PTN; (**3 – 16**) congeners isolated from SB12030.

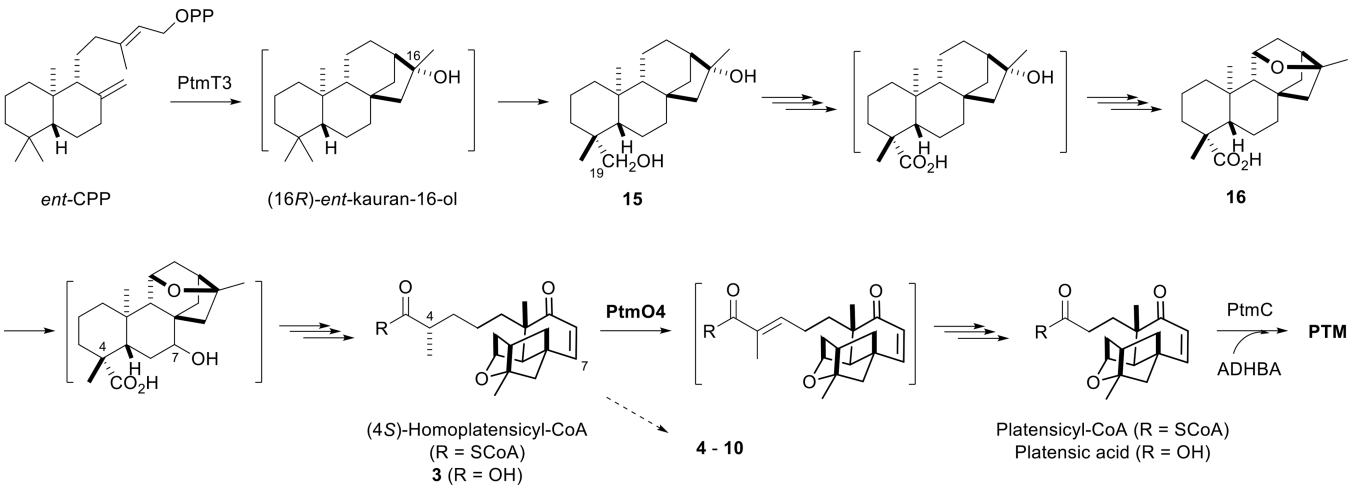

Fig. 4.

Proposed biosynthesis of PTM supported by the isolation of three intermediates (**3, 15**, and **16**) and seven congeners (**4–10**) from *S. platensis* SB12030. *ent*-CPP is first cyclized by PtmT3 to form *ent*-kauran-16-ol. The oxidation at C19 most likely occurs before the ether ring formation between C11 and C16. Hydroxylation at C7 followed by retro –aldol ring cleavage between C4 and C5 and dehydration between C6 and C7 affords the diterpenoid intermediate **3**. PtmO4, a long-chain acyl-CoA dehydrogenase, subsequently catalyzes β-oxidation of **3**, most likely in its CoA form, resulting in thiolytic loss of three carbons and formation of platensicyl-CoA. Coupling of platensicyl-CoA with 3-amino-2,4-dihydroxybenzoic acid (ADHBA) by PtmC completes the biosynthesis of PTM (**1**). Proposed intermediates in brackets have not been isolated or experimentally confirmed. Biosynthesis of PTN from *ent*-CPP parallels PTM with the exception of PtmT1-catalyzed formation of *ent*-atiserene, which undergoes similar oxidations, as supported by **11–14**, to afford platencinyl-CoA that finally couples with ADHBA to yield PTN.